AGU PUBLICATIONS

JGR

Journal of Geophysical Research: Oceans

RESEARCH ARTICLE

10.1002/2017JC012729

Observed basin-wide propagation of Mediterranean water in the Black Sea

Anastasia Falina[1], Artem Sarafanov[1], Emin Özsoy[2,3], and Ufuk Utku Turunçoğlu[4,5]

[1]P.P. Shirshov Institute of Oceanology, Moscow, Russia, [2]Eurasia Institute of Earth Sciences, Istanbul Technical University, Istanbul, Turkey, [3]Institute of Marine Sciences, Middle East Technical University, Erdemli, Mersin, Turkey, [4]Informatics Institute, Istanbul Technical University, Istanbul, Turkey, [5]Earth System Physics Section, International Centre for Theoretical Physics, Trieste, Italy

Key Points:
- Extensive propagation of Mediterranean intrusions is observed at middepths (100–600 m) in the western and eastern gyres of the Black Sea
- The main conduit for the intrusions from the Bosphorus Strait is the southern limb of the Rim Current
- Observations suggest that prominent intrusions originate from strong injections of Mediterranean water caused by strong cyclonic storms over Bosphorus

Correspondence to:
A. Falina,
falina_a@mail.ru

Citation:
Falina, A., A. Sarafanov, E. Özsoy, and U. U. Turunçoğlu (2017), Observed basin-wide propagation of Mediterranean water in the Black Sea, *J. Geophys. Res. Oceans*, *122*, 3141–3151, doi:10.1002/2017JC012729.

Received 24 JAN 2017
Accepted 2 MAR 2017
Accepted article online 7 MAR 2017
Published online 12 APR 2017

Abstract Mediterranean water entering the Black Sea through the Bosphorus Strait forms middepth intrusions that contribute to the salt, heat, and volume balances of the sea, ventilate its water column at intermediate depths and restrain the upward flux of hydrogen sulfide from deeper layers. Despite the importance for the Black Sea environment, the circulation of Mediterranean-origin water in the basin is fundamentally underexplored. Here we use hydrographic data collected from ships and Argo profiling floats to identify pathways of the Mediterranean intrusions in the general circulation system of the sea. While earlier the intrusions were observed primarily near the Bosphorus Strait, we present an evidence for their intermittent extensive propagation throughout the basin. We find that the main conduit for the intrusions is the southern limb of the Rim Current that carries the intruded water from the Bosphorus Strait eastward. A part of this eastward flow recirculates cyclonically into the interior of the sea, where traces of the intrusions gradually disappear because of mixing. We put forward the hypothesis that the formation of the most prominent intrusions is associated with strong cyclonic storms over the Bosphorus Strait, which lead to abnormally large influx of Mediterranean water.

1. Introduction

The Black Sea is one of the most isolated seas from the ocean. The near-isolation, along with a strong vertical stratification, has led to formation of a thick column of vertically stagnant anoxic water in the Black Sea from about 150 m depth to the bottom [*Neretin et al*., 2006]. Hydrographic properties of this water column are stable on seasonal to interdecadal timescales and almost uniform laterally along isopycnal surfaces [*Mamaev et al*., 1994]. Against the background of this water column, a body of intruded water of external origin can be efficiently identified and traced by its anomalous properties. This makes the Black Sea an ideal natural laboratory for studying pathways of injected water in a nearly closed deep basin.

The only link of the Black Sea to ocean-connected basins is the narrow (0.7–3.5 km) and shallow (<100 m) Bosphorus Strait that provides a waterway to the Mediterranean Sea via the Marmara Sea and the Dardanelles. The density-driven water exchange through the Bosphorus is conducted by a two-layer current system: in the upper current, low-salinity low-density water flows out of the Black Sea, while the lower current supplies the Black Sea with more saline dense water of Mediterranean origin (hereinafter MOW, the Mediterranean-origin water) [*Marsigli*, 1681; *Bogdanova*, 1963; *Latif et al*., 1991; *Özsoy et al*., 1993, 1998]. The MOW influx is crucial for the environment of the sea, as it provides salt to maintain the salinity balance at intermediate and deep levels [*Murray et al*., 1991, 2007], contributes to maintaining the main pycnocline [*Glazer et al*., 2006a; *Murray et al*., 2007] and the isothermal layer at the depths of 500–650 m [*Ivanov and Samodurov*, 2001], and ventilates the water column below the pycnocline [*Buesseler et al*., 1991; *Konovalov et al*., 2003; *Delfanti et al*., 2014]. The lateral flux of oxygen associated with MOW is thought to restrain the upward flux of hydrogen sulfide from the anoxic water column [*Konovalov et al*., 2005].

At the northern exit of the Bosphorus Strait, the salinity of MOW is nearly twice as large as the salinity of waters in the Black Sea [*Özsoy et al*., 1993]. Yet, the main identification feature of MOW in the Black Sea is the anomalous temperature rather than salinity [*Falina et al*., 2007]. After passing through the strait, warm saline MOW (12–15°C, 35–37 psu) rapidly mixes with fresher ambient water, mostly with water derived from

the Cold Intermediate Layer (CIL, $<8°C$, 18–19 psu) [*Latif et al*., 1991; *Buesseler et al*., 1991; *Özsoy et al*., 1993, 2001; *Stanev et al*., 2001]. The mixing strongly reduces salinity and density of MOW and leads to formation of MOW-derived lenses and "fingers" collectively referred to as the MOW/Bosphorus plume [*Konovalov et al*., 2003; *Glazer et al*., 2006b]. Hereinafter, along with the general term "plume," we use the term "MOW intrusion" referring to an individual body of water (of any kind: lenses, fingers), the anomalous hydrographic properties of which result from a contribution of MOW to its formation. The MOW plume descends down the slope until the plume's density becomes equal to that of ambient water and then travels away from the formation region. As density stratification in the Black Sea is mostly controlled by salinity [*Murray et al*., 2007; *Falina et al*., 2007], the plume's descent continues until reaching the level, where ambient salinity is nearly the same as salinity of the plume. As a result, beyond the near-Bosphorus region, typical salinity anomalies associated with MOW intrusions are of the same order as the accuracy of salinity measurements (10^{-3} psu). This makes it difficult to identify the intrusions from salinity data. Temperature anomalies of the intrusions are typically an order of magnitude larger than measurement accuracy (10^{-3}°C), which allows to reliably detect the intrusions against the background of ambient temperature field [*Falina et al*., 2007].

The vertical and lateral extent of propagation of MOW intrusions in the Black Sea water column is uncertain. Observations have shown that isopycnal spreading of the intrusions occurs at middepths (100–600 m) below the CIL [*Özsoy et al*., 1993; *Konovalov et al*., 2003; *Glazer et al*., 2006b; *Falina et al*., 2007]. Model simulations likewise reproduce the propagation of MOW intrusions below the CIL at depths of less than 400–500 m [*Stanev et al*., 2001; *Özsoy et al*., 2001]. Some studies [*Murray et al*., 1991, 2007; *Dubinin and Dubinina*, 2014] have suggested, based on analysis of water mass properties and composition, that MOW possibly penetrates into deep and near-bottom layers. However, no single distinct intrusion of MOW has yet been observed below the middepth layer, and thus the question on how deep the intrusions may actually descend remains open. Laterally, besides the vicinity of the Bosporus Strait [*Latif et al*., 1991; *Oğuz and Rozman*, 1991; *Özsoy et al*., 1993, 2001; *Özsoy and Beşiktepe*, 1995], the presence of MOW intrusions has also been detected, in the form of thin (up to 10 m thick) "fingers," in the southwestern part of the sea within ~200 km off the strait [*Konovalov et al*., 2003; *Glazer et al*., 2006b]. Propagation of MOW intrusions on larger distances was evidenced by only one hydrographic survey that revealed a few unexpectedly (up to 80 m) thick MOW lenses in the eastern gyre of the sea [*Falina et al*., 2007].

The pathways of MOW intrusions from the Bosphorus are unclear, as well as the mechanisms controlling their properties and propagation. It has been shown that the MOW transport in the Bosphorus Strait is subject to strong temporal variability [*Özsoy et al*., 1998; *Jarosz et al*., 2011; *Altıok et al*., 2014; *Book et al*., 2014]. Depending on atmospheric conditions over the strait the amount of MOW injected into the Black Sea may either drop to zero or increase by up to 3–4 times relative to a long-term mean [*Jarosz et al*., 2011]. Whether and to what extent this transport variability translates into variability of properties and propagation of MOW intrusions in the Black Sea remains unknown.

In this study, by analyzing data from research vessels and Argo profiling floats, we provide the first basin-scale overview of the Mediterranean water propagation and evolution in the Black Sea. We present a circulation scheme showing the main pathways of MOW intrusions from the Bosphorus Strait into the Black Sea interior. We suggest a mechanism of how the MOW plume manifestation in the Black Sea depends on atmospheric conditions over the Bosphorus region and the associated transport variability in the Bosphorus Strait.

The manuscript is organized as follows. In section 2, we examine the spatial extent of the MOW propagation over the basin. The most prominent MOW intrusions detected from Argo data are discussed in section 3. We then analyze the origin of prominent intrusions in section 4 and their propagation pathways in section 5. We conclude the paper in section 6.

2. Extent of the MOW Propagation as Observed From Ships and Floats

To investigate the spatial extent of the MOW plume propagation, we first analyzed ship-based CTD (conductivity-temperature-depth) measurements across the Black Sea interior. The data were collected from the R/V "Akvanavt" in April and August 2008, R/V "Bilim" in April 2008, and R/V "Professor Shtokman" in March 2009 (Figure 1). The majority of the CTD profiles extend to depths of 450–550 m thus covering most of the

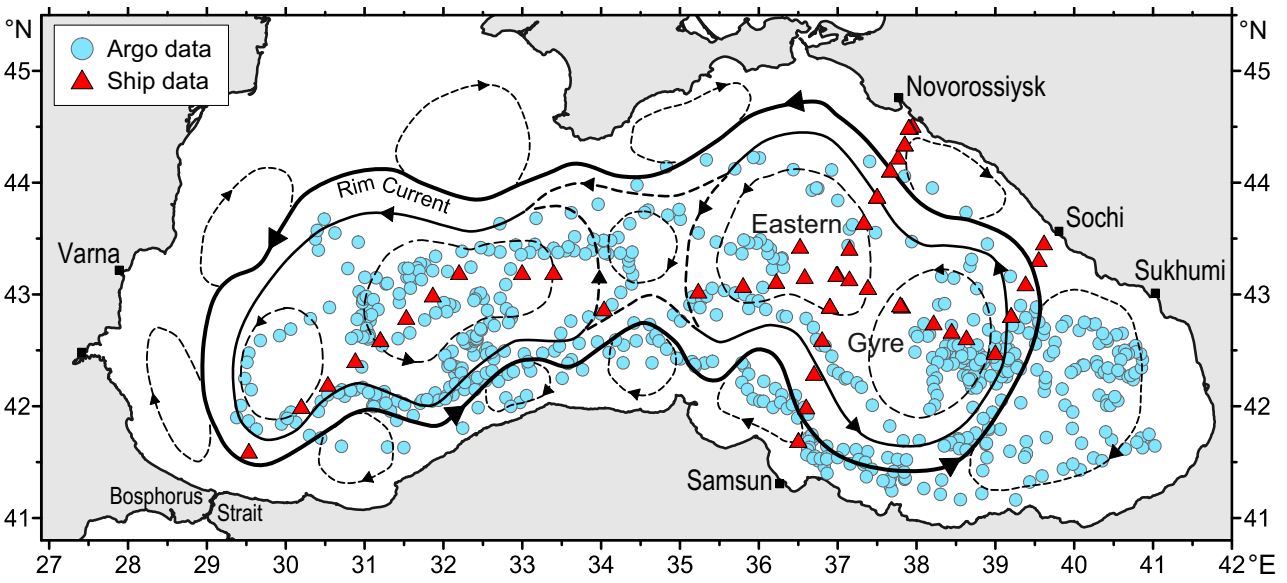

Figure 1. Hydrographic data used in the study. Locations of CTD profiles obtained from ships (2008–2009) and Argo profiling floats (2005–2009) are shown with the triangles and circles, respectively. The upper layer circulation [*Oğuz et al.*, 1993] is sketched.

middepth water column. About 20% of the profiles reach depths of ~2000 m. The accuracy of temperature and salinity measurements was better than 0.002°C and 0.002 psu, respectively.

Since the MOW plume can be reliably identified by temperature anomalies at intermediate depths [*Falina et al.*, 2007], we searched for such anomalies on every CTD profile below 100 m down to the deepest measurement. At the first step, the data were inspected in the potential temperature (θ)-salinity (S) space (see Figure 2b). The θ-S curves based on data from most of the profiles are smooth, indicating gradual evolution of temperature with density/depth (gray curves in Figure 2b). The curves are nearly overlapping despite the corresponding profiles were collected in different parts of the sea. This pattern reflects the basin-scale lateral near-homogeneity of the Black Sea's intermediate and deep waters in the distance-density space. Such profiles and the state of the water column they depict will hereinafter be referred to as "undisturbed". The profiles with the anomalies were identified by distinct irregularities in the θ-S curves (color curves in Figure 2b) deviating from the bunch of the undisturbed curves at densities corresponding to intermediate depths. Then, the magnitudes of the anomalies ($\Delta\theta$) were estimated, for each anomalous profile, as the maximum difference of potential temperature between the profile and a mean profile obtained by averaging data from 8 to 10 spatially closest undisturbed profiles. The estimates were performed using potential density (referenced to the sea surface, σ_0) as a vertical coordinate. In the θ-S space, the $\Delta\theta$ values thus obtained represent the largest along-isopycnal departures of the anomalous curves from the undisturbed ones. To ensure the reliability of the results, only $\Delta\theta$ values of $>$0.01°C, which substantially (more than 5 times) exceed the accuracy of measurements, were recognized as being associated with true anomalies.

The anomalies were detected on 12 of total 45 profiles collected in the deep (off-shelf) part of the sea (bottom depths of $>$200 m). The anomalies occupy the depth range of about 100–550 m. Note that the maximum depth of the observed anomalies (~550 m) is strongly determined by the fact that only a minor fraction (~20%) of the ship data extend below this depth. All the anomalies are positive; their magnitudes reach 0.1°C. The anomalies are scattered over nearly the whole area of observations (Figure 2a): from the vicinity of the Bosphorus Strait (sta. 1 in Figure 2) to as far east as ~38.5°E. The majority of the anomalous profiles (10 out of 12) were observed in the eastern part of the sea: in the eastern gyre interior and in the Rim Current (see Figure 1) to the north of Samsun.

The thickness of the MOW intrusions as derived from the observed anomalies varies from tens to more than hundred meters (Figure 2b). For instance, a 145 m thick intrusion ($\Delta\theta = 0.03$°C) occupying the 245–390 m

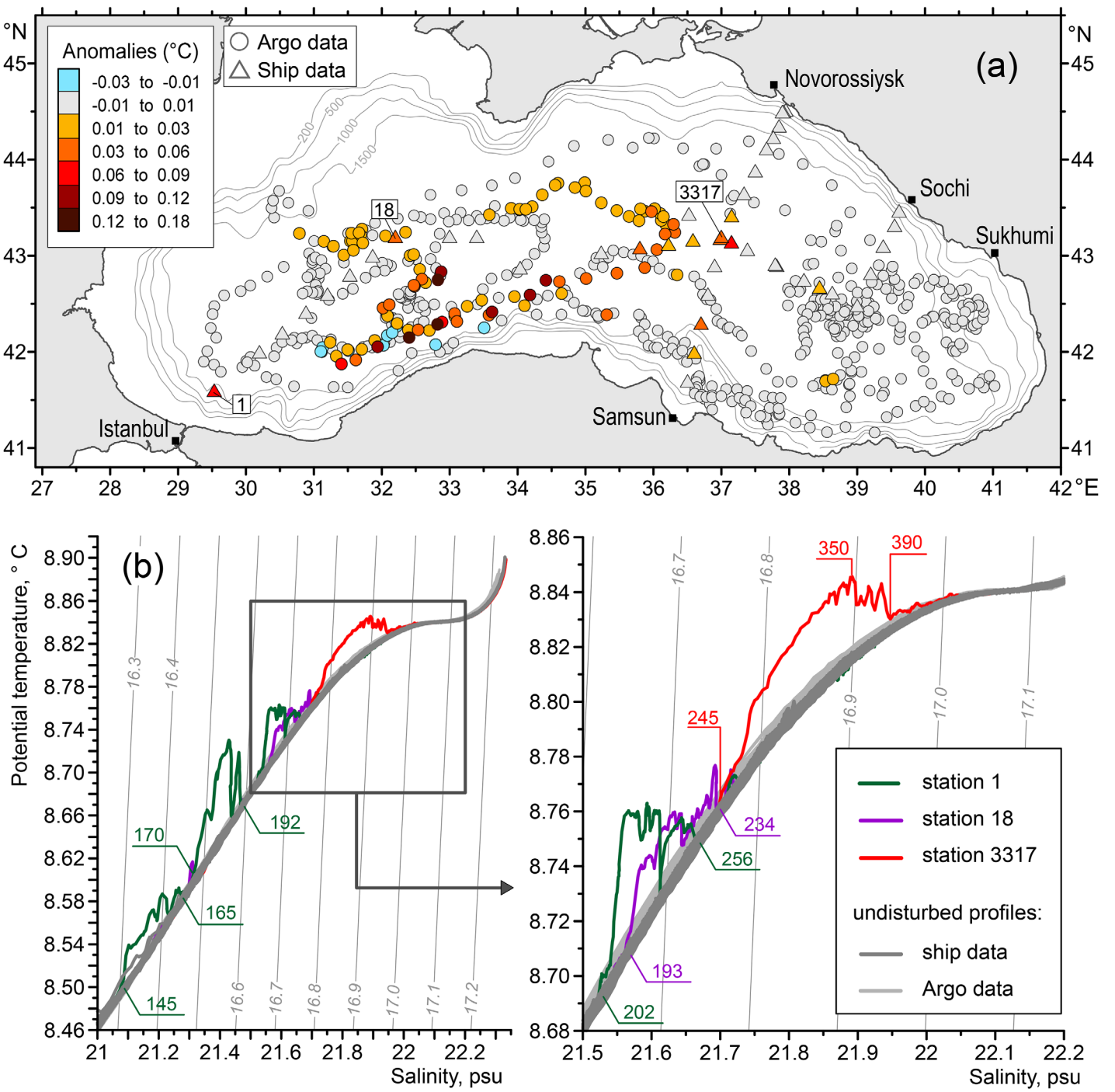

Figure 2. Middepth potential temperature anomalies. (a) About 17% of the profiles exhibit temperature anomalies exceeding 0.01°C in the 100–600 m depth range. When several anomalies occur on a single profile, the maximum anomaly was plotted. (b) The anomalies are seen in the potential temperature (θ) versus salinity (S) space as departures from undisturbed background state of the water column. The right-hand plot is an enlarged view of the θ-S range marked in the left-hand plot with the rectangle. The colored θ-S curves showing the examples of typical anomalies are based on data from stations 1, 18 (R/V "Bilim," April 2008) and 3317 (R/V "Akvanavt," April 2008). The stations are marked in Figure 2a. The depths (m) corresponding to the selected breakpoints on the curves are indicated. The nearly overlapping gray curves represent the undisturbed water column: they are based on data from ship and Argo float (float 4900541, see section 3) profiles that do not show distinct anomalies. The σ_0 isopycnals are shown with the gray lines.

depth range was found in the eastern basin (sta. 3317 in Figure 2). This substantially exceeds the thickness of the plume fingers (<10 m) observed earlier in the southwestern part of the sea [*Konovalov et al.*, 2003; *Glazer et al.*, 2006b].

In general, the ship data acquired in 2008 and 2009 show the extensive propagation of MOW intrusions, confirming and extending earlier observations by *Falina et al*. [2007]. The ship-based measurements are, however, scarce and do not provide enough data coverage to reconstruct the propagation of the intrusions between the locations where the anomalies were found.

To extend the analysis, we employed CTD data collected from Argo profiling floats in 2005–2009 (Figure 1). The chosen time span includes that of the ship-based surveys and the preceding 3 years to ensure the possibility of tracking the MOW intrusions observed from ships in the eastern basin back to the southwestern part of the sea. The Argo data (612 profiles) are from four floats (4900489, 4900540, 4900541, and 4900542) that drifted at about 1500 m depth and every 7 days ascended to the sea surface, transmitted data to satellite and then dived back to the depth of drift. When ascending, the floats measured temperature, salinity, and pressure thereby providing CTD profiles similar to those collected from ships. In the deep part of the basin, all the profiles extend to ~1500 m depth.

Each Argo profile was inspected using the same approach as for the ship data. As a result, we found 99 profiles (of total 612) with distinct temperature anomalies ($\Delta\theta > 0.01$°C) in the depth range of about 100–600 m. Most of the anomalies (~90%) are positive. The largest anomalies (up to ~0.16°C, Figure 2a) are accompanied by detectable anomalies of salinity (0.01–0.02 psu, no figure shown). Negative anomalies were detected only at 9 profiles in the western basin (Figure 2a). Intrusions that are colder than the ambient water have earlier been observed near the Bosphorus Strait [*Oğuz and Rozman*, 1991; *Özsoy et al*., 1993; *Glazer et al*., 2006b]. The mechanism responsible for the coexistence of warm and cold intrusions remains unclear. The anomalies detected in the Argo float data are discussed in more detail in section 3.

The revealed spatial distribution of the middepth potential temperature anomalies (Figure 2a) evidences the extensive propagation of MOW intrusions from the Bosphorus and implies advective connections between the southwestern part of the sea and its interior. The MOW intrusions are observed in all main elements of the general circulation system of the sea: in the Rim Current, in the western and eastern gyres and in interior flows between them (see Figures 1 and 2a). With respect to the vertical limits of the MOW propagation, none of the hundreds of the deep-reaching (Argo) profiles exhibited temperature anomalies below 600 m. This supports the notion that the propagation of MOW intrusions as recently formed distinct bodies of water with anomalous properties is confined to intermediate depths [e.g., *Özsoy et al*., 1993; *Konovalov et al*., 2003; *Glazer et al*., 2006b; *Falina et al*., 2007].

3. Intrusions Registered by an Argo Float in 2007–2009

Here we consider the temperature anomalies observed by Argo float 4900541 during its travel in the western and eastern basins of the sea (inset in Figure 3a). The data collected by the float provide a compelling example of the MOW manifestation in the water column. Two of the three intrusions encountered by the float are among the most prominent intrusions seen in our data, and are of particular importance for further discussion.

The deepest anomalies (depths 300–600 m), although not being the largest ones, are clearly seen in the distribution of potential temperature measured by the float (Figure 3b) due to a relatively weak vertical stratification of temperature below 300–400 m. Shallower anomalies (depths 100–300 m) are poorly visible in the temperature field, being represented mostly by uplifts of isotherms rather than by distinct patches of anomalously warm water. To expose these anomalies, we constructed a field of along-path differences between the observed temperature distribution and that corresponding to a reference undisturbed state of the water column (Figure 3c). The reference along-path distribution of temperature was obtained by excluding the profiles with anomalies ($\Delta\theta > 0.01$°C) and filling the gaps that arose by linear interpolation between the nearest undisturbed profiles. This approach is justified by the basin-scale lateral near-homogeneity of the water column below the layer of seasonal variability (see the nearly overlapping undisturbed θ-S curves in Figure 2b). The mesoscale wave-shaped perturbations in the temperature field (Figure 3b) are largely due to circulation, as they are accompanied by similar perturbations of potential density surfaces (see the $\sigma_0 = 15.8$ isopycnal in Figure 3b). The latter effect was accounted for by using potential density as a vertical coordinate.

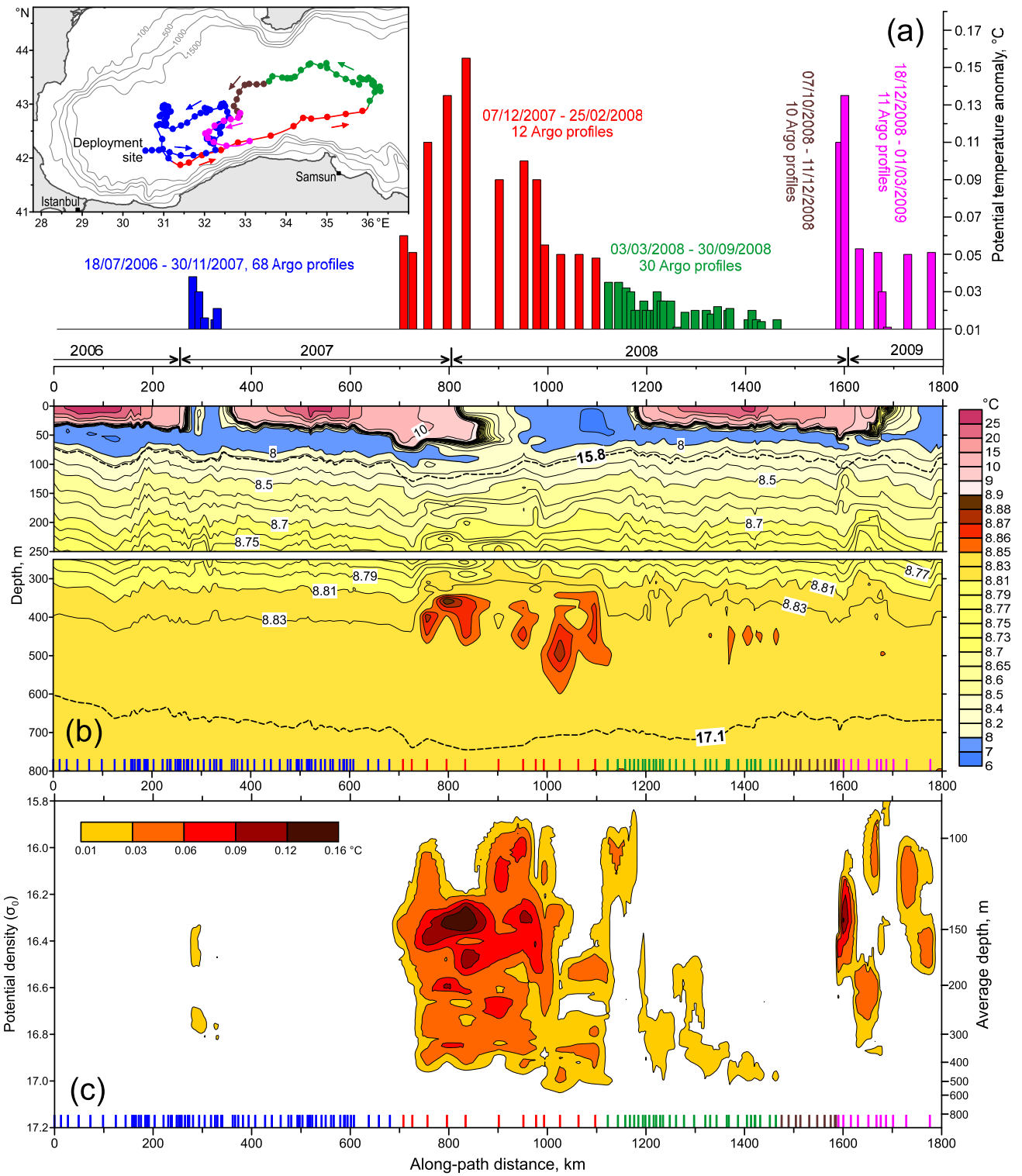

Figure 3. Middepth potential temperature anomalies observed by Argo float 4900541. (a) Anomalies (°C) as a function of distance (km) along the float's path from the deployment site. The inset shows the float's trajectory subdivided into five sequential segments according to the occurrence and magnitudes of the observed anomalies. The anomaly bars are colored the same as the corresponding segments. The time (years) of the measurements is indicated above the bottom axis. (b) Potential temperature observed by the float as a function of depth (m) and along-path distance. The dashed curves are σ_0 isopycnals 15.8 and 17.1. (c) Potential temperature anomalies relative to an undisturbed state of the water column as a function of potential density (σ_0) and along-path distance. The right-hand axis shows the average depths. In Figures 3b and 3c, the locations of the profiles are marked at the bottom axes using the same color code as in Figure 3a.

Float 4900541 was deployed in July 2006 in the western gyre of the sea (Figure 3a). The float moved eastward from the deployment site and, after a brief travel in the Rim Current, veered back into the interior of the western basin (blue segment of the float's track in Figure 3a). There, in February–March 2007, the float recorded the first relatively weak warm intrusion ($\Delta\theta < 0.04$°C, blue bars in Figure 3a) on five profiles in the 130–350 m depth range ($16.3 < \sigma_0 < 16.85$, Figure 3c). Then the float made a loop in the western gyre and, in the beginning of December 2007, re-entered the Rim Current, where it immediately encountered the second much more prominent intrusion. During the next 10 months until the end of September 2008, the float escorted the intrusion: in the Rim Current, which transported them eastward (red segment in Figure 3a), and then in the eastern gyre interior, where the flow turned back toward the western basin (green segment in Figure 3a). The largest temperature anomalies associated with the intrusion ($0.04 < \Delta\theta < 0.16$°C) were observed in the Rim Current in the 100–600 m depth range ($15.8 < \sigma_0 < 17.1$, Figure 3c). The anomalies gradually decreased along the float's pathway through the eastern basin and completely vanished when the float returned to the western interior of the sea. After the next 2.5 months (October–mid-December 2008), during which no anomalies were detected (brown segment in Figure 3a), the float again observed strong middepth temperature anomalies (depths 100–400 m, $15.8 < \sigma_0 < 16.9$, Figure 3c) and continued observing them until the end of the float's operation in the beginning of March 2009 (magenta segment in Figure 3a). These latter anomalies were registered by the float within 60 km to the north of the Rim Current and, at the two last profiling locations, directly in the Rim Current (Figure 3a). This, along with the large magnitudes of the anomalies ($\Delta\theta$ up to 0.13–0.14°C), suggests that they were associated with a new—the third for the float—intrusion that was brought to the observation site by the Rim Current from the west.

4. Probable Origin of the Most Prominent Intrusions

Observations suggest that the propagation of detectable ($\Delta\theta > 0.01$°C) MOW intrusions over the Black Sea is an intermittent rather than continuous process. Otherwise, temperature anomalies associated with MOW would have been routinely observed, which is not the case even for the southwestern part of the sea adjacent to the Bosphorus Strait. In the latter region, only a single profile in our data set showed an intrusion (sta. 1 in Figure 2), contrary to what could be expected from earlier studies [*Latif et al*., 1991; *Oğuz and Rozman*, 1991; *Özsoy et al*., 1993, 2001; *Glazer et al*., 2006b]. Measurements in the Rim Current by Argo float 4900541 did not detect distinct anomalies when the float entered the current for the first time shortly after the deployment in 2006, while a year later, when the float revisited the current, it recorded a prominent MOW plume at the location where it was absent before (Figure 3).

The most plausible explanation for the intermittent manifestation of the MOW intrusions is the strong variability of the MOW inflow through the Bosphorus Strait (Figure 4c). Depending on the atmospheric conditions over the strait, transport of the lower current carrying MOW may vary dramatically from zero to more than 1100 km^3/yr [*Jarosz et al*., 2011], which is several times larger than the time-mean value (~300 km^3/yr) [*Ünlüata et al*., 1990; *Beşiktepe et al*., 1994; *Jarosz et al*., 2011]. The largest transports of the lower current and, hence, the strongest injections of MOW into the Black Sea are associated with events of blockages and reversals of the upper current in the strait [*Jarosz et al*., 2011; *Altıok et al*., 2014; *Book et al*., 2014]. These events, locally known as "Orkoz," are caused by strong southerly winds that occasionally push the upper-layer water in the strait northward with enough force to stop and reverse the upper current [*Beşiktepe et al*., 1994; *Jarosz et al*., 2011; *Altıok et al*., 2014]. As a result, the entire water column in the strait moves toward the Black Sea, and the lower current transport substantially increases. The Orkoz events typically last for 2–3 days and occur predominantly in fall and winter [*Beşiktepe et al*., 1994; *Jarosz et al*., 2011; *Altıok et al*., 2014].

The observations of the two major MOW intrusions by Argo float 4900541 (Figure 3) were preceded by atmospheric conditions over the Bosphorus Strait, which are typical of the Orkoz events. In one of the two cases, the circulation changes in the strait were documented from direct current measurements [*Jarosz et al*., 2011; *Book et al*., 2014].

An event of the upper current reversal and the associated increase in the lower current transport in the Bosphorus Strait (Figure 4c) was observed during a remarkably strong cyclonic storm that passed over the strait on 21–22 November 2008 [*Jarosz et al*., 2011; *Book et al*., 2014]. The storm had many devastating consequences, including the sinking of Kadıköy Pier in the Bosphorus Strait in Istanbul [*Book et al*., 2014]. Atmospheric pressure at Istanbul sharply dropped by 30 hPa (down to 984 hPa, Figure 4b) and southerly wind

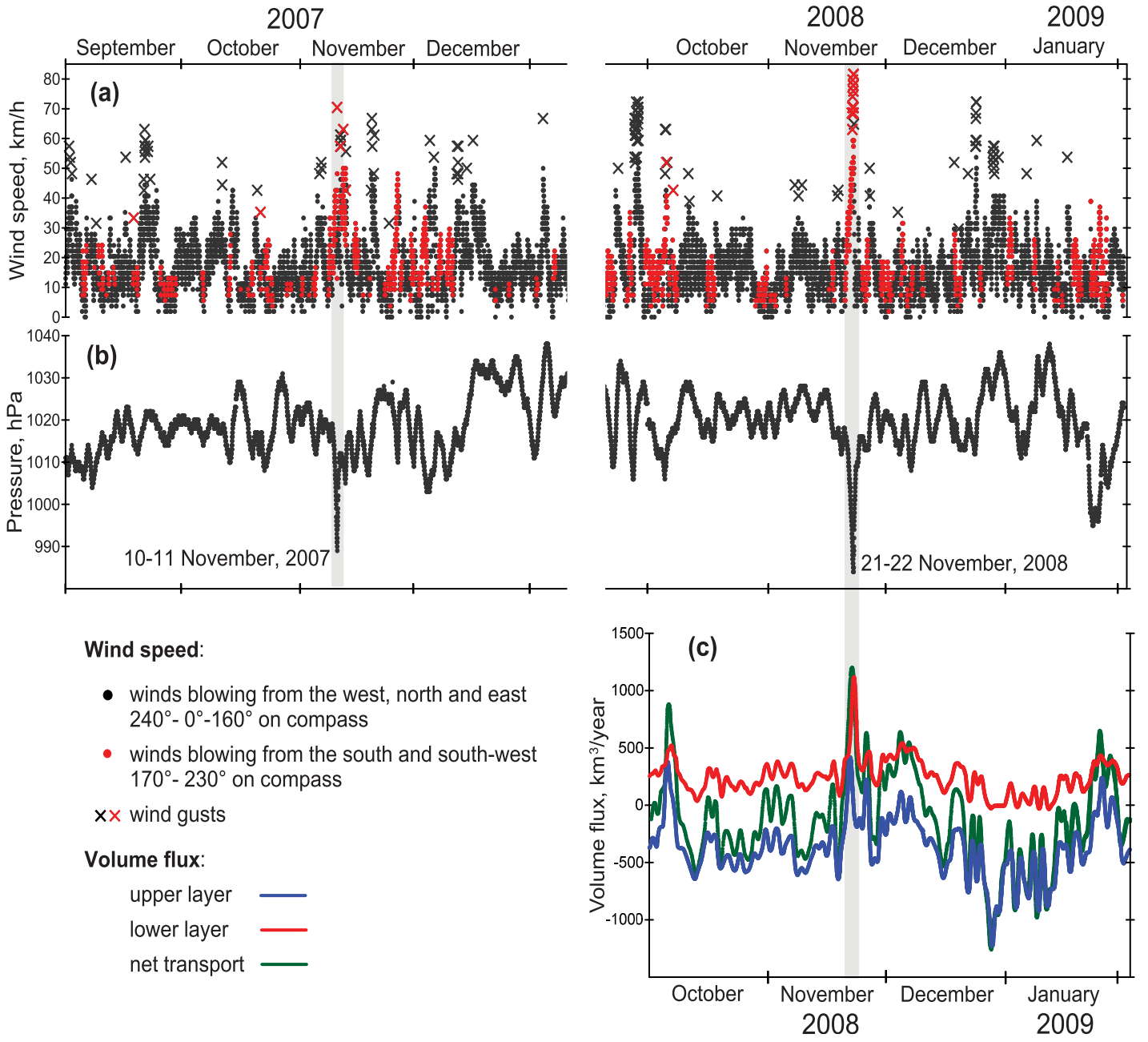

Figure 4. Dependence of transport through the Bosphorus Strait on atmospheric conditions. (a and b) Time series of (a) wind speed and (b) atmospheric pressure at Istanbul. (c) Transport time series based on moored current measurements at the northern exit of the Bosphorus Strait [*Jarosz et al.*, 2011]. Positive transports are toward the Black Sea. The gray vertical bands mark the major events of strong southerly winds (southerly wind gusts of 60–80 km/h), low atmospheric pressure (980–990 hPa), and anomalously large transport to the Black Sea in the lower layer (>1000 km^3/yr).

gusts reached speeds of up to 80 km/h (Figure 4a). The circulation in the strait rapidly responded to this forcing: the flow of the Black Sea water to the Marmara Sea in the upper layer was blocked and reversed [*Jarosz et al.*, 2011], velocity of the lower current (typically 40 cm/s) increased to 200 cm/s [*Book et al.*, 2014], and the peak values of the lower current transport exceeded 1100 km^3/yr (Figure 4c) [*Jarosz et al.*, 2011]. Accordingly, the storm led to a short-term anomalously strong injection of MOW into the Black Sea. Nearly a month after the injection, on 18 December 2008, the prominent MOW intrusion was encountered by float 4900541 in the Black Sea interior (Figure 3). The distance from the Bosphorus Strait to the location where the intrusion was observed (300–400 km along the Rim Current) and the time between the injection and the detection of the intrusion (~1 month) suggest a possibility that the intrusion observed by the float

originated from the injection (which, in turn, was caused by the storm). Indeed, to reach the observation site, the intrusion would have to propagate from the strait with an average speed of 10–15 cm/s, which is consistent with typical velocities in the Rim Current at intermediate depths [*Korotaev et al*., 2006].

Similarly to the above case, a strong cyclonic storm passed over the Bosphorus Strait (on 10-11 November 2007, Figure 4) about a month before the float encountered the thick intrusion in the Rim Current on 7 December 2007 (Figure 3). During the storm, atmospheric pressure at Istanbul dropped down to 988 hPa (Figure 4b) and the southerly wind gusts reached 60–70 km/h (Figure 4a). The storm crossed the Black Sea toward the Sea of Azov and had catastrophic consequences: 10 ships sank or ran aground, two tankers were damaged, resulting in the death of 23 sailors and a major oil spill. Whether the storm caused an increase in transport of the lower current in the Bosphorus Strait remains unknown in the absence of transport measurements for that time period. Assuming that the dynamic response of the circulation in the strait was similar to that observed during the storm in November 2008, it is likely that a strong injection of MOW into the Black Sea did occur. That would explain the appearance of the MOW intrusion in the Rim Current in December 2007.

We thus hypothesize that the most prominent MOW intrusions in the Black Sea are generated by the impact of extremely strong cyclonic storms on the circulation in the Bosphorus Strait. Strong southerly winds associated with a storm may block the upper current and cause a drastic increase in transport of the lower current in the strait. This results in a short-term injection of an anomalously large amount of warm saline MOW into the Black Sea and to the formation of a prominent MOW intrusion. Anomalously high temperatures of such intrusions allow to detect them in hydrographic data at large distances from the formation region. Testing the hypothesis will require additional observations, including longer transport time series in the Bosphorus Strait. Additionally, the testing would benefit of employing a numerical model capable of reproducing the transport variability in the strait in response to atmospheric forcing, as well as realistic circulation and mixing in the Black Sea.

5. Pathways of Intrusions

The spatial pattern of the observed temperature anomalies (Figure 1b) allows to depict the propagation pathways of MOW intrusions in the general circulation system of the sea (Figure 5). To better understand

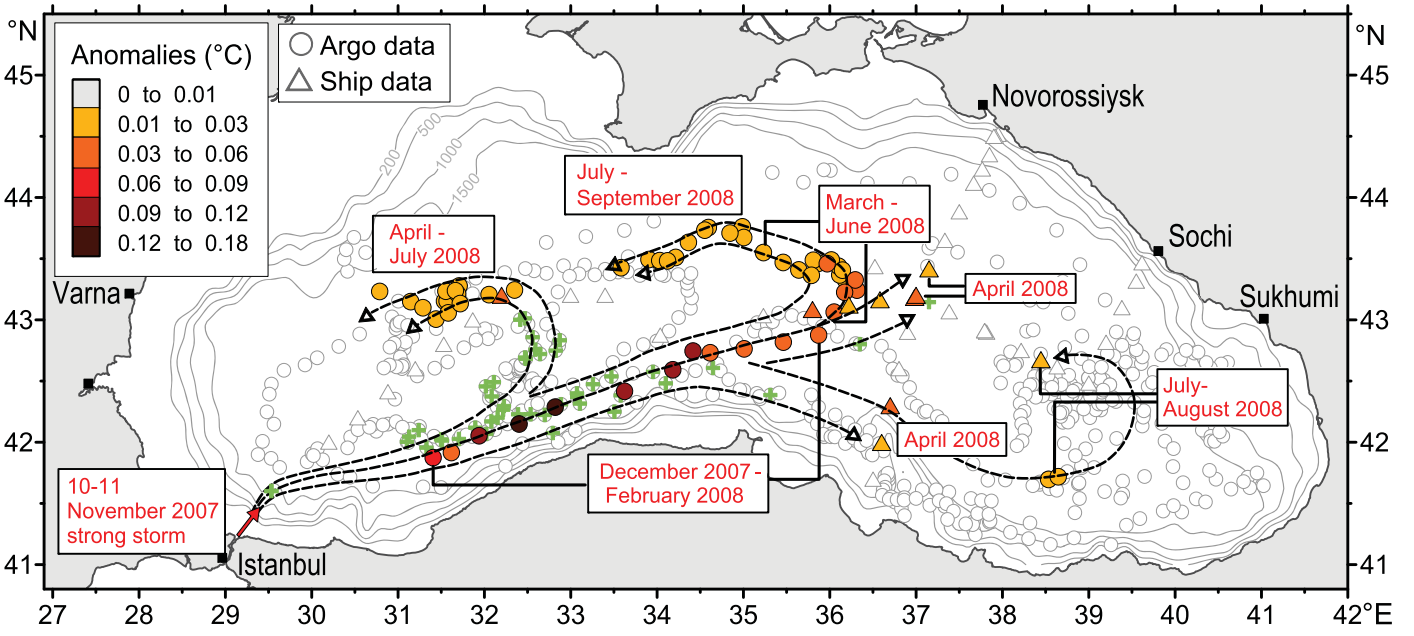

Figure 5. Pathways of Mediterranean-origin intrusions from the Bosphorus Strait into the Black Sea interior as inferred from the observed middepth temperature anomalies. The color circles and triangles show the anomalies ($\Delta\theta > 0.01$°C) associated with the prominent intrusion that appeared in the sea after the strong storm over the Bosphorus on 10–11 November 2007. The months when the anomalies were observed are labeled. The locations of all other anomalies ($\Delta\theta > 0.01$°C) detected in the present study (Figure 2a) are marked with the green crosses.

the along-path evolution of the anomalies and the approximate propagation times, we put the emphasis on the anomalies observed between the two strong storms that occurred over the Bosphorus Strait on 10–11 November 2007 and 21–22 November 2008 (Figure 4). The occurrence of these anomalies in time and space (color circles and triangles in Figure 5) strongly suggests that they were associated with a single prominent MOW intrusion that, as we hypothesized above, originated from a strong injection of MOW through the strait during the storm in November 2007 and then was propagating over the Black Sea during almost a year. The intrusion was first observed in December 2007 in the western part of the Rim Current southern limb (~41.8°N, ~31.5°E). The Rim Current transported the intrusion eastward, and it took the intrusion almost 1.5 months to reach the eastern basin (east of 34°E). On the path through the western basin, a part of the flow turned cyclonically from the Rim Current into the interior of the western gyre, where the intrusion was observed in April–July 2008. In the eastern basin, the flow diverged. A part proceeded in the Rim Current to the southeast toward the easternmost part of the sea, where (east of 38°E) the intrusion was observed in July–August 2008. The other part of the flow entered the interior of the eastern gyre in February–March 2008. There, the flow split into two branches: the one directed to the center of the gyre, where (43–43.5°N, 37–37.5°E) the intrusion arrived by April 2008, and another one that turned cyclonically to the west and reached the interface between the eastern and western gyres (~43.5°N, ~34°E) in July–September 2008. The latter pathway was observed by a single float (4900541) all the way from the southwestern part of the sea (Figure 3).

The magnitude of anomalies generally exhibits a basin-scale decline in the direction of the flow (Figure 5), which is an apparent consequence of along-path mixing with colder ambient water. The largest anomalies ($\Delta\theta$ up to 0.10–0.16°C) were observed in December 2007 to January 2008 in the western part of the Rim Current (west of 34.5°E). From there, the anomalies generally decreased downstream, until they completely disappeared by the end of summer 2008.

The circulation pathways as described above are inferred from the observations covering a relatively short time period (less than a year) and hence should not be regarded as persistent, stationary pathways of MOW intrusions. Given that the circulation varies on many temporal and spatial scales, these pathways may also considerably vary in time. Nonetheless, the anomalies detected in the rest of our data set (green crosses in Figure 5) suggest a recurrent appearance of the intrusions along the revealed pathways: in the Rim Current and in the western and eastern gyres. To shed more light on the extent of temporal variability of the MOW pathways, more observations and possibly numerical simulations are needed.

6. Conclusion

The present analysis suggests that the most prominent middepth (100–600 m) MOW intrusions in the Black Sea originate from strong injections of Mediterranean water during strong cyclonic storms over the Bosphorus Strait. Such intrusions propagate in the Black Sea over much larger area than was previously reported. The main conduit for the intrusions is the southern limb of the Rim Current, which within several months delivers the intrusions to the eastern and western gyres of the sea. Temperature anomalies associated with an intrusion decrease in magnitude due to mixing and become undetectable in less than a year after the intrusion departed from the Bosphorus Strait. In line with earlier studies that have suggested the propagation of MOW intrusions within the intermediate layer [*Özsoy et al*., 1993; *Konovalov et al*., 2003; *Glazer et al*., 2006b; *Falina et al*., 2007], the present analysis shows no signatures of intrusions below 600 m.

Author Contribution

A.F. designed the study. A.F. and A.S. analyzed the Argo and Russian ship data and wrote the manuscript. E.Ö. and U.U.T. analyzed the Turkish ship data. All authors contributed extensively to interpretation of the results.

Author Information

The authors declare no competing financial interests. Correspondence and requests for materials should be addressed to A.F. (falina_a@mail.rumailto).

Acknowledgments
We thank Andrey Zatsepin, Vyacheslav Kremenetskiy, and Alexander Dubinin for the data from the R/Vs "Akvanavt" and "Professor Shtokman." The ship data from April 2008 were collected within the framework of the European Integrated Project (036949) "Southern European Seas: Assessing and Modelling Ecosystem Changes (SESAME)." The meteorological data are from https://www.wunderground.com, and the Argo float data are from http://www.coriolis.eu.org. We thank Sergey Konovalov and a second anonymous reviewer for their comments that helped to improve the manuscript.

References

Altıok, H., A. Aslan, S. Övez, N. Demirel, A. Yüksek, N. Kıratlı, S. Tas, A. E. Müftüoğlu, H. I. Sur, and E. Okuş (2014), Influence of the extreme conditions on the water quality and material exchange flux in the Strait of Istanbul, *J. Mar. Syst.*, *139*, 204–216, doi:10.1016/j.jmarsys.2014.06.005.

Beşiktepe, Ş. T., H. I. Sur, E. Özsoy, M. A. Latif, T. Oğuz, and Ü. Ünlüata (1994), The circulation and hydrography of the Marmara Sea, *Prog. Oceanogr.*, *34*(4), 285–333, doi:10.1016/0079-6611(94)90018-3.

Bogdanova, A. K. (1963), The distribution of Mediterranean waters in the Black Sea, *Deep Sea Res. Oceanogr. Abstr.*, *10*(5), 665–672.

Book, J. W., E. Jarosz, J. Chiggiato, and Ş. T. Beşiktepe (2014), The oceanic response of the Turkish Straits System to an extreme drop in atmospheric pressure, *J. Geophys. Res. Oceans*, *119*, 3629–3644, doi:10.1002/2013JC009480.

Buesseler, K. O., H. D. Livingston, and S. A. Casso (1991), Mixing between oxic and anoxic waters of the Black Sea as traced by Chernobyl cesium isotopes, *Deep Sea Res., Part II*, *38*, S725–S745, doi:10.1016/s0198-0149(10)80006-8.

Delfanti, R., E. Özsoy, H. Kaberi, A. Schirone, S. Salvi, F. Conte, C. Tsabaris, and C. Papucci (2014), Evolution and fluxes of ^{137}Cs in the Black Sea/Turkish Straits System/North Aegean Sea, *J. Mar. Syst.*, *135*, 117–123, doi:10.1016/j.jmarsys.2013.01.006.

Dubinin, A., and E. Dubinina (2014), Isotope composition of oxygen and hydrogen in the Black Sea waters as a result of the dynamics of water masses, *Oceanology*, *54*(6), 713–729, doi:10.1134/S0001437014050038.

Falina, A., A. Sarafanov, and I. Volkov (2007), Warm intrusions in the intermediate layer (150–500 m) of the Black Sea eastern gyre interior, *Geophys. Res. Lett.*, *34*, L22602, doi:10.1029/2007GL031016.

Glazer, B. T., G. W. Luther III, S. K. Konovalov, G. E. Friederich, D. B. Nuzzio, R. E. Trouwborst, B. M. Tebo, B. Clement, K. Murray, and A. S. Romanov (2006a), Documenting the suboxic zone of the Black Sea via high-resolution real-time redox profiling, *Deep Sea Res., Part II*, *53*, 1740–1755, doi:10.1016/j.dsr2.2006.03.011.

Glazer, B. T., G. W. Luther III, S. K. Konovalov, G. E. Friederich, R. E. Trouwborst, and A. S. Romanov (2006b), Spatial and temporal variability of the Black Sea suboxic zone, *Deep Sea Res., Part II*, *53*, 1756–1768, doi:10.1016/j.dsr2.2006.03.022.

Ivanov, L. I., and A. S. Samodurov (2001), The role of lateral fluxes in ventilation of the Black Sea, *J. Mar. Syst.*, *31*(1–3), 159–174, doi:10.1016/s0924-7963(01)00051-3.

Jarosz, E., W. J. Teague, J. W. Book, and S. Beşiktepe (2011), Observed volume fluxes in the Bosphorus Strait, *Geophys. Res. Lett.*, *38*, L21608, doi:10.1029/2011GL049557.

Konovalov, S. K., et al. (2003), Lateral injection of oxygen with the Bosporus plume—Fingers of oxidizing potential in the Black Sea, *Limnol. Oceanogr. Methods*, *48*(6), 2369–2376, doi:10.4319/lo.2003.48.6.2369.

Konovalov, S. K., J. W. Murray, and G. W. Luther III (2005), Basic processes of Black Sea Biogeochemistry, *Oceanography*, *18*(2), 24–36, doi:10.5670/oceanog.2005.39.

Korotaev, G., T. Oğuz, and S. Riser (2006), Intermediate and deep currents of the Black Sea obtained from autonomous profiling floats, *Deep Sea Res., Part II*, *53*, 1901–1910, doi:10.1016/j.dsr2.2006.04.017.

Latif, M. A., E. Özsoy, T. Oğuz, and Ü. Ünlüata (1991), Observations of the Mediterranean inflow into the Black Sea, *Deep Sea Res., Part A*, *38*, S711–S724, doi:10.1016/S0198-0149(10)80005-6.

Mamaev, O. I., V. S. Arkhipkin, and V. S. Tuzhilkin (1994), TS-analysis of the Black Sea waters, *Oceanology*, *34*(2), 154–168.

Marsigli, L. F. (1681), *Osservazioni Intorno al Bosforo Tracio overo Canale di Constantinopoli rappresentate in Lettera alla Sacra Real Maesta Cristina Regina di Svezia da Luigi Ferdinando Marsigli*, Nicolo Angelo Tinassi, Roma.

Murray, J. W., Z. Top, and E. Özsoy (1991), Hydrographic properties and ventilation of the Black Sea, *Deep Sea Res., Part A*, *38*, S663–S689, doi:10.1016/S0198-0149(10)80003-2.

Murray, J. W., K. Stewart, S. Kassakian, M. Krynytzky, and D. DiJulio (2007), Oxic, suboxic and anoxic conditions in the Black Sea, in *The Black Sea Flood Question: Changes in Coastline, Climate, and Human Settlement*, edited by V. Yanko-Hombach et al., pp. 1–21, Springer, Dordrecht, Netherlands.

Neretin, L. N., I. I. Volkov, A. G. Rozanov, T. P. Demidova, and A. S. Falina (2006), Biogeochemistry of the Black Sea anoxic zone with a reference to sulphur cycle, in *Past and Present Water Column Anoxia*, edited by L. N. Neretin, pp. 69–104, Springer, Dordrecht, Netherlands, doi:10.1007/1-4020-4297-3_04.

Oğuz, T., and L. Rozman (1991), Characteristics of the Mediterranean underflow in the southwestern Black Sea continental shelf/slope region, *Oceanol. Acta*, *15*(5), 433–444.

Oğuz, T., V. S. Latun, M. A. Latif, V. V. Vladimirov, H. I. Sur, A. A. Markov, Özsoy, E., B. B. Kotovshchikov, V. V. Eremeev, and Ü. Ünlüata (1993), Circulation in the surface and intermediate layers in the Black Sea, *Deep Sea Res., Part I*, *40*, 1597–1612, doi:10.1016/0967-0637(93)90018-X.

Özsoy, E., and Ş. Beşiktepe (1995), Sources of double diffusive convection and impacts on mixing in the Black Sea, in *Double-Diffusive Convection, Geophysical Monograph 94*, edited by A. Brandt and H. J. S. Fernando, pp. 261–274, AGU, Washington, D. C.

Özsoy, E., Ü. Ünlüata, and Z. Top (1993), The evolution of Mediterranean water in the Black Sea: Interior mixing and material transport by double diffusive intrusions, *Prog. Oceanogr.*, *31*, 275–320, doi:10.1016/0079-6611(93)90004-W.

Özsoy, E., M. A. Latif, Ş. T. Beşiktepe, N. Çetin, M. Gregg, V. Belokopytov, Y. Goryachkin, and V. Diaconu (1998), The Bosporus Strait: Exchange fluxes, currents and sea-level changes, in *Ecosystem Modeling as a Management Tool for the Black Sea, vol. 2, NATO Sci. Ser.*, edited by L. I. Ivanov and T. Oğuz, pp. 1–27, Kluwer Academic Publishers, Dordrecht.

Özsoy, E., D. Di Iorio, M. Gregg, and J. Backhaus (2001), Mixing in the Bosphorus Strait and the Black Sea Continental Shelf: Observations and a model of the dense water outflow, *J. Mar. Syst.*, *31*, 99–135, doi:10.1016/S0924-7963(01)00049-5.

Stanev, E. V., J. A. Simeonov, and E. L. Peneva (2001), Ventilation of Black Sea pycnocline by the Mediterranean plume, *J. Mar. Syst.*, *31*, 77–97, doi:10.1016/S0924-7963(01)00048-3.

Ünlüata, Ü., T. Oğuz, M. A. Latif, and E. Özsoy (1990), On the physical oceanography of the Turkish Straits, in *The Physical Oceanography of Sea Straits*, edited by L. J. Pratt, pp. 25–60, Kluwer Acad., Dordrecht, Netherlands.